Thermodynamic analysis of an integrated gasification solid oxide fuel cell plant combined with an organic Rankine cycle

Pierobon, Leonardo; Rokni, Masoud; Larsen, Ulrik; Haglind, Fredrik

Published in:
Renewable Energy

Link to article, DOI:
10.1016/j.renene.2013.05.021

Publication date:
2013

Pierobon L., Rokni M., Larsen U. and Haglind F., 2013, "Thermodynamic analysis of an integrated gasification solid oxide fuel cell plant with an organic cycle", *Renewable Energy*, Vol. 60, pp. 226–234.

Thermodynamic analysis of an integrated gasification solid oxide fuel cell plant combined with an organic Rankine cycle

Leonardo Pierobon, Masoud Rokni, Ulrik Larsen, Fredrik Haglind
Technical University of Denmark, Department of Mechanical Engineering,
Building 403, DK-2800 Kgs. Lyngby, Denmark

Abstract

A 100 kW_e hybrid plant consisting of gasification system, solid oxide fuel cells and organic Rankine cycle is presented. The nominal power is selected based on cultivation area requirement. For the considered output a land of around 0.5 km^2 needs to be utilized. Woodchips are introduced into a fixed bed gasification plant to produce syngas which fuels the combined solid oxide fuel cells – organic Rankine cycle system to produce electricity. More than a hundred fluids are considered as possible alternative for the organic cycle using non-ideal equations of state (or state-of-the-art equations of state). A genetic algorithm is employed to select the optimal working fluid and the maximum pressure for the bottoming cycle. Thermodynamic and physical properties, environmental impacts and hazard specifications are also considered in the screening process. The results suggest that efficiencies in the region of 54-56% can be achieved. The highest thermal efficiency (56.4%) is achieved with propylcyclohexane at 15.9 bar. A comparison with the available and future technologies for biomass to electricity conversion is carried out. It is shown that the proposed system presents twice the thermal efficiency achieved by simple and double stage organic Rankine cycle plants and around the same efficiency of a combined gasification, solid oxide fuel cells and micro gas turbine plant.

Keywords: Solid oxide fuel cells; Organic Rankine cycle; Gasification; Biomass; Genetic algorithm

1. Introduction

In the last decade the penetration of renewable energy into the global energy market has been increasing constantly. In March 2007, the European Union targeted 20% renewable energy for year 2020 [1], in which small scale units (less than 100 MW) play an important role. Although the major contribution is expected to be provided by wind and solar power, biomass is also going to play a key role in the future scenario. However, current biomass utilization for electric generation can further be improved in terms of thermal efficiency. Small scale steam cycle plants with electric power outputs of 10-20 MW have efficiencies of around 25-28%, while at smaller scale (5-1000 kW) organic Rankine cycle plants (ORC) and Stirling engines can be used, which also have efficiencies up to 30%.

Technologies based on wood gasification have already reached the market. They enable the conversion of lingo-cellulosic biomass into a gaseous medium that may be utilized for electric power generation combined with a fuel cells plant [2]. For example, [3] employed a fixed bed gasifier with a compact cogeneration system to cover the electrical and thermal demands in a rural area and showing an energy solution for small social communities using renewable fuels. In [4], a downdraft wood gasifier is used to produce wood gas which then burns in an internal combustion engine for cogeneration purpose.

Solid oxide fuel cell (SOFC) is an electrochemical reactor currently under development aimed at power and heat generation application. SOFC can be fed with many different gaseous fuels such as methane, natural gas and syngas. Due to the high operating temperature, light hydrocarbon fuels, (e.g. methane) can be internally reformed within the cell through reforming and water-gas shift reactions. Such high operating temperature has also been the biggest obstacle for commercialization of SOFC.

In the literature many combinations of SOFC and conventional power plants are demonstrated, for instance, in [5] for producing combined heat and power and in [6] with internal biomass gasification. Characterization, quantification and optimization of hybrid SOFC and gas turbine systems were studied in [7] and [8]. In [9] a hybrid plant producing combined heat and power from biomass by use of a two-stage gasification concept, SOFC and micro gas turbine was considered.

In hybrid SOFC and gas turbine plants the stacks must be pressurized in an extremely large vessel (depending on the size of the plant which is usually in MW class). This practical problem is diminished in hybrid SOFC and ORC or steam cycle systems, because the stacks work at atmospheric pressure. In addition, the manufactures are trying to decrease the operating temperature of the fuel cell stacks. Hence, the system would be more attractive with a steam or an organic cycle. The investigations on combined SOFC and steam cycle were pre-studied first by [10], while [11] and [12] presented an integrated system consisting of an SOFC and steam plant fired by natural gas with a thermal efficiency of 62%. A triple hybrid plant fueled by woodchips based upon gasification plant, SOFC and steam cycle is analyzed and optimized for electric power production in [13]. A reasonable size for such a biomass plant is of around 5-50 MW requiring a cultivation area of 20-125 km^2 [14]. At smaller scales (less than about 500 kW), the steam turbine isentropic efficiency decreases significantly which then in turn adversely affect the plant efficiency to sharply decrease. In addition, choosing an appropriate steam live pressure to avoid high moisture content at turbine outlet and thereby avoiding blade corrosion would be challengeable. This issue can be eluded by replacing the bottoming cycle with an organic (“dry”) fluid cycle. Furthermore, at small-scale applications (<1 MW), ORCs have a number of advantages with biomass applications such as higher thermal efficiency in full and part-load as well as higher compactness, as reported in [15]. Previous investigations, [16] presented an energetic performance analysis for a combined power generation system fed by methane consisting of SOFC and ORC running with R113. In [17] the integration of SOFC and ORC is proposed for trigeneration applications, in which n-octane was selected as ORC working media and the plant was again fuelled by methane. Such solution was also considered for use on onboard ship by [18] with an electric power production of around 250 kW_e.

The present paper aims at presenting an advanced system for electric conversion of woodchips, in which a detailed gasification plant model utilizing a mixture of steam and air as oxidant is utilized. The gasification model is based on the Viking gasifier currently in operation at the Technical University of Denmark. The gasification plant is coupled with the SOFC system and the ORC, and the target for net power production is set to 100 kW_e based on cultivation area requirements. More than a hundred working fluids for the organic Rankine cycle are screened using the genetic algorithm (GA). The optimization variables and the thermodynamic parameters are selected based, not only on thermal efficiency but also on safety, availability, health and environmental issues. Moreover, the plant is compared with the existing technologies, utilizing conversion of woodchips to electric power. In this paper the modeling approach is described in section 2. The plant layout is presented in section 3 and full results about the optimization process and system performance are reported in section 4. Results are discussed in detail in section5. Finally, in section 6 the main conclusions are outlined.

The plant presented here is named as integrated gasification SOFC and organic Rankine cycle (IGSORC). Such a concept is new and has not been studied previously. The objective of this study is to theoretically demonstrate that such a combined biomass-based energy generator offers advantages of high thermal efficiency compared to traditional power generators, but needs further development prior to industrial application, especially with respect to the fuel cell.

2. Methodology

The present section introduces first (subsection 2.1) the simulation tool utilized for the calculations. The optimization procedure is then described in subsection 2.2. Finally, subsections 2.3 and 2.4 illustrate the gasification and SOFC models.

2.1 Dynamic Network Analysis

Dynamic Network Analysis (DNA) is a simulation tool used for energy systems analysis [19]. It is the present result of an ongoing development at the Department of Mechanical Engineering, Technical University of Denmark, which began with a Master's Thesis work in 1989 [20]. Since then the program was developed to be generally applicable for covering unique features, and hence supplementing other simulation programs. In DNA the physical model is formulated by connecting the relevant component models through nodes and by including operating conditions for the complete system. The physical model is converted into a set of mathematical equations to be solved numerically. The mathematical equations include mass and energy conservation for all components and nodes, as well as relations for thermodynamic properties of the fluids involved. The program includes a component library with models for a large number of different components existing within energy systems. Components are modeled with a number of constitutive equations representing their physical properties, i.e. heat transfer coefficients for heat exchangers and isentropic efficiencies for compressors and turbines. Steady state (involving algebraic equations), dynamic (involving differential equations) simulations and exergy analysis can be conducted. The fluid library has been recently extended by linking DNA with the commercial software REFPROP 9 [21]. The source code, provided under license in FORTRAN language, is compiled together with DNA to form unique software, in which more than a hundred real media including hydrocarbon fluids are now available. The thermodynamic properties at the critical point of the working fluids relevant for context of present study as well as health hazard (HH), fire hazard (FH) and physical hazard (PH) according to the HMIS (Hazardous Materials Identification System) are listed in Table A1 in appendix A. As seen in the table, a significant amount of fluids are considered in this study, more than 100 fluids. Due to environmental concerns some fluids are phased out such as R-11, R-12, R-113, R-114 and R-115. Some other fluids are going to be banned in 2020 or 2030 for example R-21, R-22, R-123, R-124, R-141b and R142b [22] and therefore, these media are excluded from this study.

2.2 The optimization procedure

To search for the optimal organic media an optimization method is required. This is achieved by using the benefits of genetic algorithm. These benefits can be mentioned as; avoiding the calculation of derivatives and also its capability of searching for the global optimum [23]. In the GA an initial population of strings is created in which a single string stands as a possible solution to a specific task. Each solution is then evaluated by means of an objective function. A portion of the initial populations is maintained based on certain operation probabilities for crossover and mutation to produce a new generation. Fitter strings

replace the poorer strings in order to improve the overall fitness of the objective function. In the present case the objective function is the thermal efficiency of IGSORC and the two optimization variables are the ORC working fluid (an integer corresponding to a specific fluid in the DNA library) and the maximum pressure in the organic loop. The GA method is included in the MATLAB 2012a optimization toolbox, therefore, MATLAB and DNA are linked together to perform the optimization procedure as shown in Fig. 1.

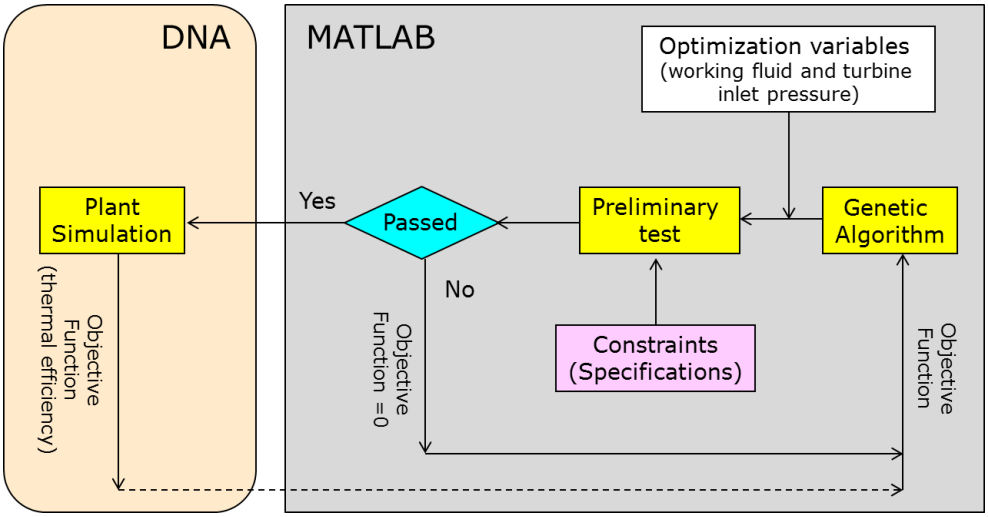

Figure 1. Schematic description of the optimization process (genetic algorithm) by linking the MATLAB code with DNA.

In MATLAB environment, the GA sets the optimization variables (working fluid and maximum turbine inlet pressure) to be investigated, see Fig. 1. Subsequently a preliminary test is performed to check the consistency of these two inputs with the constraints to be specified in the model. If the test is not passed the thermal efficiency is set to zero and the GA starts a new iteration, otherwise the plant will be simulated in DNA. Then DNA gives a signal to GA that the thermal efficiency is calculated and GA chooses a new set of optimization variables and a new iteration will be started. This procedure will be continued until the optimized values are found. To be noted that the GA parameters are set as the default values, i.e. population size 20, generation size 100, crossover fraction 0.8 and migration fraction 0.2. The following constraints are specified for the preliminary test:

a) It is verified that minimum and maximum pressure and temperature are within the limits for which the thermodynamic properties of the fluid can be calculated;
b) Since the analysis is limited to subcritical ORC, if the critical pressure is lower than the maximum pressure imposed by the GA a zero thermal efficiency is returned;
c) The lowest ORC pressure, corresponding to the temperature at the saturated liquid state, is calculated; a test on this variable is performed when a lower limit is set;
d) If the pressure input from the GA is lower than the lowest ORC pressure a zero thermal efficiency is returned;
e) Health, fire and physical hazards of the fluid are compared to the maximum allowable values; if one of the three hazards exceeds the limits the thermal efficiency is set to zero.

2.3 Gasifier modeling

To model the gasifier a general Gibbs reactor is used, meaning that the total Gibbs free energy has its minimum when the chemical equilibrium is achieved [24]. This characteristic is used to calculate the outlet gas composition at a specified temperature and pressure without

considering the reactions paths. An option for adjusting the CH_4 level in the equilibrium composition is included which can be used to calibrate the product gas compositions against the experimental results. Such modeling procedure is general and can be used for any type of gasifier as long as the syngas compositions from the considered gasifier are known. Further details can be found in [13].

The gasification process used in this study is based on the two-stage Viking gasifier. It is a 75 kW_{th} gasifier which was built in 2002 at Risø–Technical University of Denmark and results are reported in [25]. The pyrolysis and gasification processes are divided into two separate reactors, as shown in Fig. 2. Wet biomass (woodchips) is introduced into the first reactor where drying and pyrolysis take place before the pyrolysis products (600°C) are fed to the second reactor; a downdraft fixed bed char gasifier. The exhaust gases from the gasifier are then used to heat the reactor for drying and pyrolysis (see the steam loop in Fig. 2). Between pyrolysis and char gasification, partial oxidation of the pyrolysis products provides the heat for the endothermic char gasification reactions. Chars are gasified in the fixed bed while H_2O and CO_2 act as gasifying agents in the char gasification reactions. The Viking gasifier operates nearly atmospheric pressure.

2.4 Solid oxide fuel cell modeling

The SOFC model used in this investigation is based on the work presented in [26]. For the sake of clarity it is shortly described. The model computes the efficiency of the cell by means of Eq. (1).

$$\eta_{SOFC} = \eta_{rev}\eta_v U_F \tag{1}$$

where the utilization factor U_F is assumed as parameter while the reversible efficiency η_{rev} is the maximum theoretical efficiency expressed in Eq. (2) as the ratio between the change in Gibbs free energy $\Delta\bar{g}_f$ and the change in enthalpy of formation $\Delta\bar{h}_f$. Both terms are associated with full oxidation of the fuel.

$$\eta_{rev} = \left.\frac{\Delta\bar{g}_f}{\Delta\bar{h}_f}\right|_{Full\ Oxidation} \tag{2}$$

The voltage efficiency η_v is a measure of the electrochemical performance of the SOFC and it is defined as

$$\eta_v = \frac{E - \Delta V_{act} - \Delta V_{ohm} - \Delta V_{conc}}{E} \tag{3}$$

where E is the Nernst potential and ΔV_{act}, ΔV_{ohm} and ΔV_{conc} are the activation, ohmic and concentration voltage losses.

The activation overpotential is due to an energy barrier (activation energy) that the reacting species must overcome in order to drive the electrochemical reactions. The activation overpotential of each electrode is a non-linear function of the current density and is usually expressed by the Butler-Volmer equation [27]. The total activation overpotential in this model is hereby defined as the sum of the activation overpotential of each electrode, anode and cathode.

The ohmic overpotential is caused by the ohmic resistance towards the oxygen ions passing through the electrolyte and the electrons passing through the electrodes and

interconnects. The ohmic overpotential is dominated by the resistance in the ion conducting electrolyte. The temperature-dependent correlation for the ionic conductivity of the electrolyte is taken from, see e.g. [28].

The concentration overpotential is a result of the limitations of diffusive transport of reactants and products between the flow channel and the electrode-electrolyte interface. The effect is increasing with current density and at a certain current density limit this transport of species is not fast enough to feed the electrochemical reactions taking place and the partial pressure of reactants at the electrode-electrolyte interface approaches zero. The anode and cathode current density limits are different and they are dependent on microstructural characteristics of the respective electrode and operating conditions of the SOFC, see e.g. [28].

3. Plant Configuration

3.1 Integrated gasification, solid oxide fuel cells and organic Rankine cycle (IGSORC)

The combination of the gasification process with SOFC and ORC results in the plant configuration presented in Fig. 2. Wet woodchips with 33.2% moisture content (molar base) are supplied to the two-stage gasification plant for wood gas production. The first reactor accounts for the drying and pyrolysis processes while the second reactor is a fixed bed gasifier. The drying process is crucial when it comes to decrease woodchips moisture content. Herein the woodchips moisture is decreased to 0.5% from the original 33.2%. As reported in [29], the product gas is pure enough to be fed to the SOFC cells without any problem. However, in this study a simple hot gas cleaner is used to remove the small amount of sulfur which may exists after the gasifier. The operating temperature of the desulfurizer is assumed to be about 240°C. The cleaned wood gas is then preheated in a heat exchanger (AP; anode preheater) to 650°C before entering to the anode side of the SOFC stacks. The operating temperature of the SOFC stacks as well as its outlet temperatures is assumed to be 780°C. The burned fuel after the stacks is used to preheat the incoming fuel to the anode preheater. On the other side of the fuel cell, air is compressed and preheated in a heat exchanger (CP; cathode preheater) to 600°C before entering the cathode side of the SOFC stacks. Due to utilization factor of the SOFC cells, some fuel is still left after the anode side of the SOFC stacks. The off-fuel together with the off-air coming out of the cathode side is thus sent to a burner for further combustion. The off gases from the burner are sent into an intermediate heat exchanger (IHE) wherein DOWTHERM Q is used as an intermediate fluid for heat transfer. The absorbed heat is then conveyed to the ORC through the heat recovery steam generator (HRSG) consisting of three heat exchangers of super heater (SUP), evaporator (EVA) and economizer (ECO). The organic fluid is first heated up to saturated liquid in the economizer, then vaporized in the evaporator and finally superheated before expanding in an ORC turbine. An internal recuperator is added into the ORC cycle to preheat the liquid produced after the condensation and pumping processes using the exhaust vapor after the turbine. Such technique is proved to increase the system performance, see e.g. [30]. It can be noted that the energy of the off-gases exiting the IHE is further utilized in a hybrid recuperator (HR) to preheat the compressed air prior to SOFC and therefore recycling the off-heat back into the system and increase the plant efficiency accordingly, as described in [12].

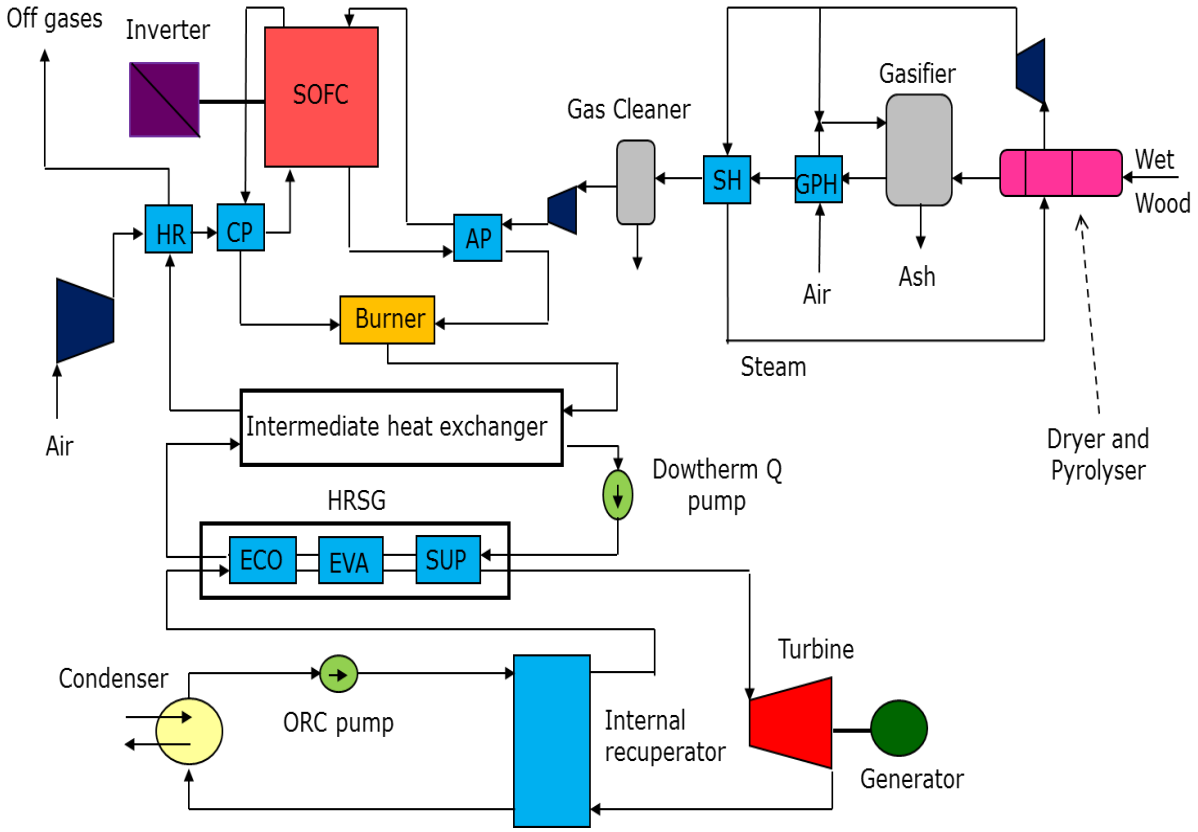

Fig. 2. Plant layout for the integrated gasification, SOFC and organic Rankine cycles.

3.2 Size of the plant

When biomass is used as energy source restriction due to cultivation area must be considered. To calculate the area of cultivation needed by a generic biomass to produce a certain amount of electric power the following equation can be adopted

$$A_{cultivation} = k \frac{36\, P_{el}\, H}{\eta_{th} \beta_{cultivation} LHV} \tag{4}$$

where thermal efficiency η_{th} is defined as

$$\eta_{th} = 100 \frac{P_{el} - P_{aux}}{\dot{m}_{fuel}\, LHV} \tag{5}$$

k–factor is a dimensionless coefficient (>1) considering street, houses, new planted area and the area wherein plants are growing. P_{el}, H, η_{plant}, and $\beta_{cultivation}$ are the plant electrical power [MW_e], operating hours per year, plant efficiency and annual productivity of the land [ton/ (ha year)]. LHV is the lower heating value of the wet biomass.

It was assumed that the plant is running on 7000 hours per year (H = 7000) while the annual productivity of the cultivation area was assumed to be $\beta_{cultivation}$ = 35 [ton.ha^{-1}year^{-1}]. The dimension for the calculated cultivation area, $A_{cultivation}$, would be in km^2. The dimensionless coefficient k larger than unity is included in order to consider additional occupied area such as new planted trees, non-grown plants, streets, etc. In order to be on the safe side, k = 4 was assumed in this study. If P_{el} = 100 kW and η_{plant} = 0.55 [16],[17],[18] then the corresponding cultivation area would be about 0.46 km^2.

The properties of woodchip are assumed to be the same as reported in [25] namely; C = 48.8%, O = 43.9%, H = 6.2%, S = 0.02%, N = 0.17% and ashes = 0.91%. The validity of the gasifier model with these compositions was studied in [13]. Depending on the time of the year moisture content up to 60% can be encountered resulting in decreased plant power input. In calculations a dried based lower heating value of 18.28 MJ/kg and a heat capacity of 1.35 kJ/kgK are assumed [25]. A moisture content of 33.2% is then added on top of these values leading to a humid based lower heating value of 11.4 MJ/kg. Moisture content has major effect on heating value of the fuel and therefore it has a significant effect on plant performance in terms of efficiency and power production. Such effect was investigated by [31] in detail and therefore will not further be studied here. For additional information the reader is referred to [31]. A major parameter is the ash content that may cause high cost of disposal along problems associated with fouling and corrosion of the fluid-bed gasifier that could occur when chlorine and sulfur traces are present which have the capability of forming hydrochloric and sulfuring acid [14].

3.3Intermediate loop

The ORC working fluid is typically a carbon- or hydrogen-based media. Off gases exiting the SOFC cathode has a substantial oxygen content which implies that a direct heat exchange with an organic media could substantially increase the risk of fire or explosion in case of leakage. To avoid this issue an intermediate loop is placed between the ORC and the heat source (c.f. Fig. 2). Furthermore, this solution enhances the thermal inertia of the bottoming cycle facilitating start up and part-load operations. In the present study a glycol-based fluid named DOWTHERM Q is selected as the intermediate fluid. It presents better thermal stability, low viscosity and higher heat transfer coefficient compared to hot oils [32]. DOWTHERM Q is modeled as an incompressible fluid for which the detailed equations are reported in [33].

4. Results

4.1 Screening of working fluids

Table 1 lists the main parameters assumed in the simulations. It can be noted that the same amount of woodchips (0.016 kg/s), i.e. cultivation area, is considered. Such assumption equalizes the energy input in the system when different fluids are investigated. It must be noted that the upper and lower temperature limits of DOWTHERM Q fluid are 360°C and -35°C respectively. A prudential value of 335°C is assumed for the maximum temperature, while no problems are encountered for the low temperature. As reported in [15], the turbine inlet temperature must not exceed 600 K (327°C) to ensure the chemical stability of the working fluid which implies that the temperature of the organic fluid at the superheater outlet shall be fixed to 320°C. Maximum process pressure is limited to 20 bar to reduce safety measures and material expenses [15], [30]. Considering the size of the plant the turbine isentropic efficiency is set to 80% and the mechanical efficiency of the pump is fixed at 80%. [30].

Table 1. Integrated gasification, SOFC and organic Rankine cycle parameters utilized in the simulations.

Parameter	Value
Wood chips temperature	15 [°C]
Wood chips mass flow	0.016 [kg/s]
Dry wood temperature	150 [°C]

Gasifier mean operating temperature	800 [°C]
Gasifier pressure drop	0.05 [bar]
Gasifier carbon conversion factor	1
Gasifier non-equilibrium methane	0.01
Steam blower isentropic efficiency	80 [%]
Steam blower mechanical efficiency	98 [%]
Steam temperature in the steam loop	150 [°C]
Wood gas blower isentropic efficiency	80 [%]
Wood gas blower mechanical efficiency	98 [%]
Gas cleaner pressure drop	0.0049
Compressor air inlet temperature	15 [°C]
Compressor isentropic efficiency	80 [%]
Compressor mechanical efficiency	98 [%]
SOFC cathode inlet temperature	600 [°C]
SOFC anode inlet temperature	650 [°C]
SOFC operating temperature	780 [°C]
SOFC utilization factor	0.85
SOFC current density	300 [mA/cm^2]
Heat exchangers fuel side pressure drops	0.008 [bar]
Heat exchangers air side pressure drops	0.008 [bar]
Burner pressure drop	5 [%]
IHE DOWTHERM Q side pressure drops	0.15 [bar]
IHE gas side pressure drops	0.008 [bar]
IHE DOWTHERM Q outlet temperature	335 [°C]
IHE pinch point	10 [°C]
DOWTHERM Q and ORC pump mechanical efficiency	80 [%]
ORC turbine isentropic efficiency	80 [%]
Superheater outlet temperature	320 [°C]
Evaporator pinch point	5 [°C]
ORC internal recuperator pinch point	5 [°C]
Condenser outlet temperature	25 [°C]

Using the parameters listed in Table 1 along with the description in subsection 2.2, the GA is initiated by fixing the maximum pressure range (1-20 bar), together with the maximum health hazard (<3), fire hazard (<4) and physical hazard (<2). The fluid number, which corresponds to a specific fluid in the DNA library, varies from 101 (acetone) to 171 (RC318). Two optimizations are performed: the first one does not have any restriction in the minimum pressure while the second one sets the lower limit to 0.05 bar according to [15]. When a temperature of 25°C is imposed at the condenser outlet, then different minimum pressures for each organic fluid are obtained. The lower the pressure is, the more challenging and expensive it would be to avoid the introduction of air in the organic loop. Limiting the minimum pressure to 0.05 bar enhances the feasibility of the plant, although some fluids that are more suitable, may be excluded during the preliminary test operation (see subsection 2.2).

4.2 Without restriction on minimum pressure of ORC cycle

Having no restriction on minimum pressure of ORC cycle, the results are presented in Table 2. The best three candidates are identified as propylcyclohexane, decane and nonane, among which the highest plant efficiency of 56.4% is achieved by propylcyclohexane as organic fluid with optimal turbine inlet pressure of 15.9 bar. However, the other two best candidate, decane and nonane could also be used as working fluid in the ORC loop with plant

efficiencies that are slightly lower than the one with propylcyclohexane, (0.2%-points respective 0.4%-points lower).

Table 2. Optimal fluids and maximum ORC pressure for the integrated gasification, SOFC and organic Rankine cycle. No constraints are set for the minimum pressure in the organic loop.

Fluid	**Propylcyclohexane (C3CC6)**	**Decane**	**Nonane**
Condenser outlet pressure [bar]	0.006	0.002	0.006
Turbine inlet pressure [bar]	15.9	12.5	16.5
Average mean temperature [°C]	266.6	265.5	261.7
ORC thermal efficiency [%]	36.2	35.8	35.5
Net power output [kW]	108.1	107.8	107.6
IGSORC thermal efficiency [%]	56.4	56.2	56.0

Figure 3 shows the temperature vs. heat exchanged between the off gases and the best three working fluids nominated for the ORC loop. Heat is first transferred from the off gases to the intermediate loop and thereafter from the DOWTHERM Q to the bottoming cycle. Propylcyclohexane presents the highest mean thermodynamic temperature (as shown in Table 2), and therefore the Carnot efficiency with this fluid is maximized. This benefit allows for achieving the highest overall thermal efficiency of the plant. Propylcyclohexane, decane and nonane have a high critical temperature of 630.8K, 617.7K and 594.6K respectively (see Table A1 in appendix A). Hence for a given inlet turbine pressure, a higher evaporation temperature can be obtained, which in turn allows the heat to be provided at higher temperature level and consequently the Carnot efficiency will be enhanced. In this sense the importance of the hybrid recuperation will be crucial. In fact, even if the temperature of the off gases exiting the IHE is high (300-350°C), the heat will be recycled back into the plant through the hybrid recuperator instead of being wasted to the ambient.

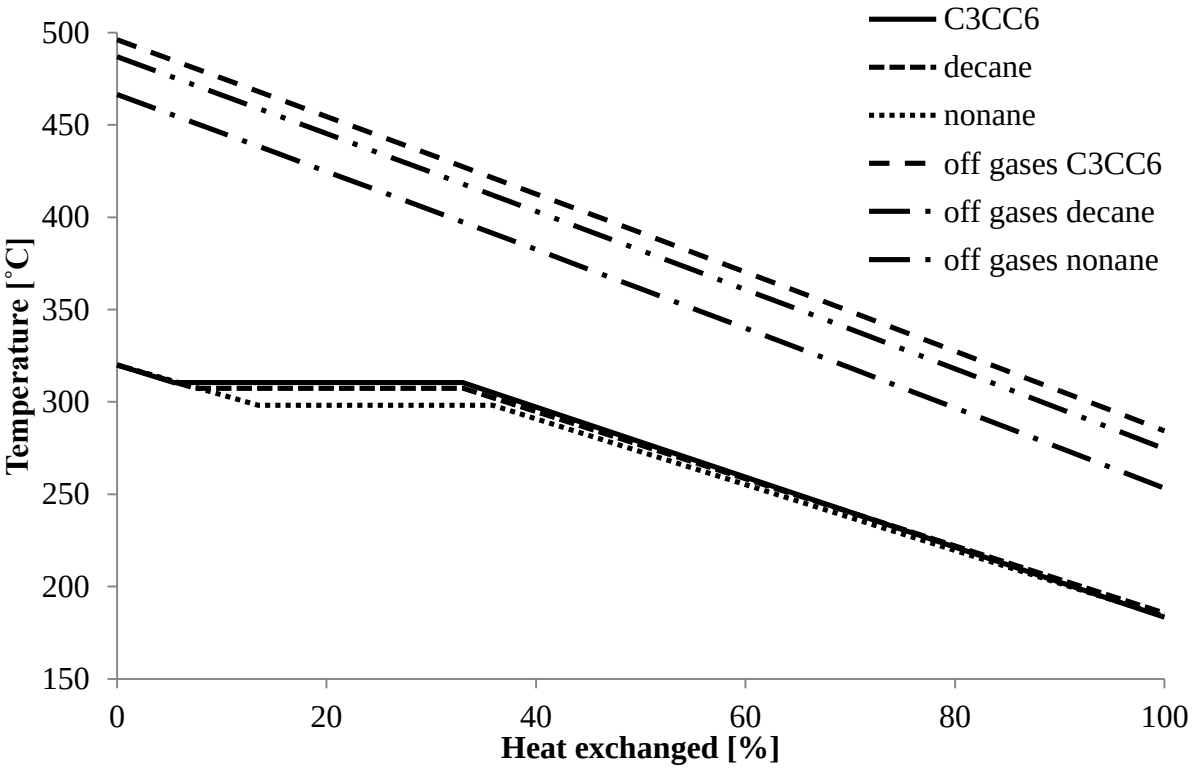

Figure 3. Off-gases temperatures of propylcyclohexane (C3CC6), decane and nonane vs. heat exchanged in a T-Q diagram. No constraints are set for the minimum pressure in the organic loop. Heat is exchanged first in the IHE (off gases-DOWTHERM Q) and then in the HRSG (DOWTHERM Q-organic fluid).

4.3 With restriction on minimum pressure of ORC cycle

In the second simulation the condensation pressure is limited to 0.05 bar. The detailed results are reported in Table 3. In this case, the best ORC fluid is cyclohexane with an optimal turbine inlet pressure of 20.0 bar. The system performance is 55.2%. The second and third preferable alternatives are hexane and cyclopentane, as shown in Table 3.

Table 3.Optimal fluids and maximum ORC pressure for the integrated gasification, SOFC and organic Rankine cycle. Lowest minimum pressure in the organic loop is set to 0.05 bar.

Fluid	**Cyclohexane**	**Hexane**	**Cyclopentane**
Condenser outlet pressure [bar]	0.13	0.202	0.423
Turbine inlet pressure [bar]	20.0	20	20.0
Average mean temperature [°C]	239.3	237.7	216.7
ORC thermal efficiency [%]	33.5	32.8	31.1
Net power output [kW]	106.0	105.5	104.0
IGSORC thermal efficiency [%]	55.2	54.8	54.1

The critical temperatures for cyclohexane, hexane and cyclopentane are 553.6K, 507.8K and 511.7K respectively. Figure 4 shows the temperature path of the organic media and the respective off-gas for the three fluids versus heat exchanged (T-Q diagram). Highest thermal efficiency and net power output are obtained with cyclohexane as working media. This can also be seen by inspecting the T-Q diagram in Fig. 4, where the area between the temperature of off-gas line and the temperature of ORC line represents the exergy destruction. Such exergy destruction (area) is the smallest one for the case of cyclohexane as ORC medium. Table 3 reports also the minimum pressures for the three ORCs (pressure after the condenser). The highest minimum pressure (0.423 bar) is obtained with cyclopentane as working fluid.

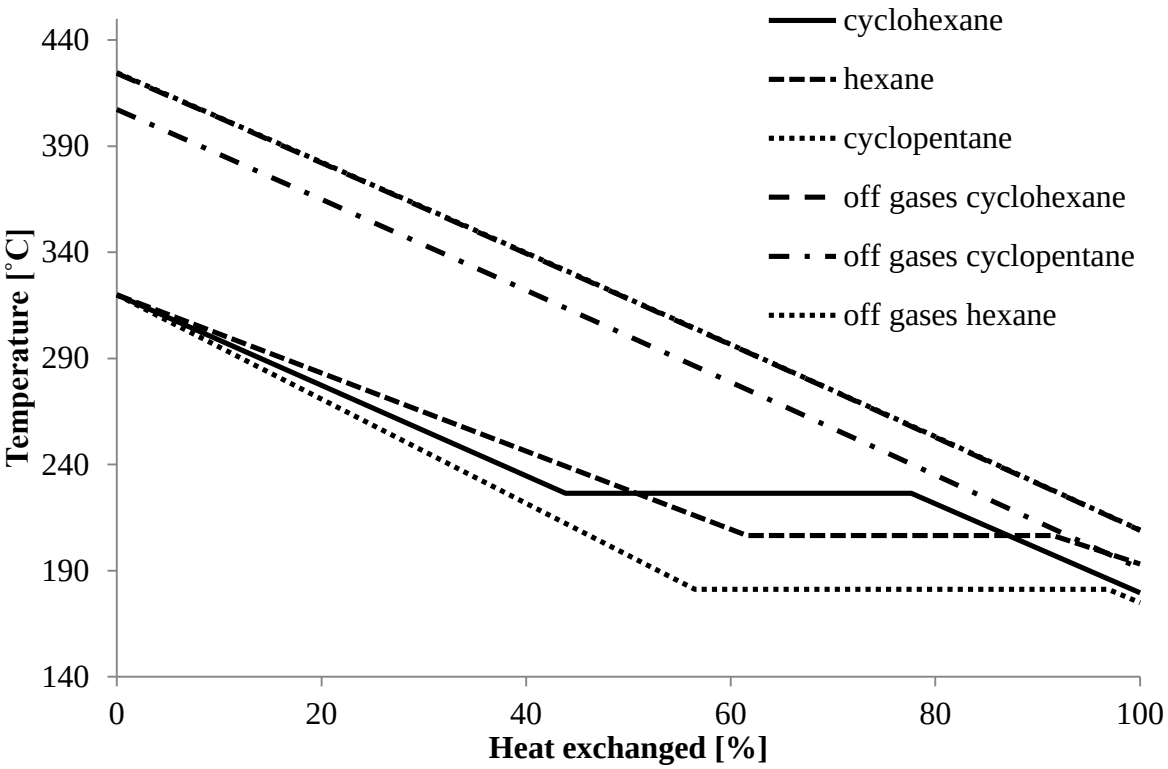

Figure 4. Off-gases temperatures of cyclohexane, hexane and cyclopentane vs. heat exchanged in a T-Q diagram. Lowest minimum pressure in the organic loop is set to 0.05 bar. Heat is exchanged first in the IHE (off gases-DOWTHERM Q) and then in the HRSG (DOWTHERM Q-organic fluid).

4.4 Optimized system and future scenario

Based on the results presented in the previous section, an optimized system is thus proposed in which propylcyclohexane is selected as the working fluid in the ORC for further investigation. Furthermore, utilization factor and current density of SOFC are set to 0.9 and 100 mA/cm^2 respectively as the result of optimization investigation presented in [12]. In addition, the turbine inlet pressure is assumed to be 15.9 bar in the simulations. The results of such optimized system are presented in Table 4. In the ongoing SOFC development, operating temperature is expected to decrease in order to reduce the investment cost [12] and therefore, simulations for two operating temperatures of 780°C (current development) and 650°C (future scenario) are performed; the results are presented in Table 4. As can be noted, with the current technology (780°C) a plant efficiency of 62.9% is obtained, while for the future scenario (650°C) the plant efficiency will be 55.3%. A drop of 7.6 % points is obtained as a result of decreasing the operating temperature of the SOFC cells. This efficiency is still very high compared to the traditional technology. The obtained results are in line with the study of [13] in which a steam cycle was used as a bottoming cycle.

Table 4. Main outputs for the optimized system and for future scenario in the case of the integrated gasification, SOFC and organic Rankine cycle.

Results	**Optimized system**	**Future scenario**
Cells operating temperature	780 [°C]	650 [°C]
Net power output [kW]	119.6	106.7
SOFC power output [kW]	95.7	78.9
ORC power output [kW]	23.8	27.7
SOFC Nernst voltage [V]	0.882	0.720

ORC thermal efficiency [%]	36.5	35.7
Overall thermal efficiency [%]	62.9	55.3

The efficiency drop due to the lowering of the operating temperature of SOFC stacks is partially because of higher irreversibility (lower electrolyte conductivity) in SOFC cells which in turn decreases the cell voltages as well as power produced by SOFC stacks. Consequently, the thermal efficiency of the IGSORC cycle will decrease since the heat rejected from the topping is increased when cell operating temperature is lowered.

5. Discussion

The performance of the presented IGSORC is compared with the available data in the literature (both present and future technologies) for the electric power conversion of woodchips. The integration of gasification and gas engine analyzed in [25] has a thermal efficiency of 25.0%. Hence, the IGSORC can potentially increase the system performance of 26.4%-points. Based on the results reported in [15] and [34], simple and double stage ORCs fired by woodchips present a poor thermal efficiency (25.3% and 34.8%) compared to the IGSORC (56.4%). At similar power output (scale), the integration of gasification with SOFC and a recuperated micro gas turbine studied in [9] presents a thermal efficiency of 55.0%. Hence, it competes well with the presented IGSORC in terms of system performance. Combined cycle integrated with a gasification plant have a thermal efficiency of 46.8% [35] but they are not applicable for the targeted net power output of this study since the lowest values reported in open literature refers to 8 MW_e systems, which is significantly higher compared to the target of this study (kW class). Furthermore, it shall be noted that the overall performance of gasification, SOFC and steam cycle plant reported in [13] differs slightly (only 0.4%-points lower) from the IGSORC efficiency presented here. Regarding the selection of the best working fluid for the ORC, the results reported in section 4 suggest that fluids with high critical temperature are required to achieve a high thermal efficiency. The hexane family (propylcyclohexane, cyclohexane and hexane) is an optimal group for an IGSORC application.

6. Conclusions

A woodchips gasification plant integrated with a SOFC and an ORC plant is presented and thermodynamically analyzed. A net power output of 100 kW_e with a cultivation area of about 0.5 km^2 is considered. The working fluid and inlet turbine pressure in the organic loop are selected with the genetic algorithm by setting constraints on maximum and minimum ORC pressure, health, fire and physical hazards. The results suggest that optimal fluid in terms of system performance is propylcyclohexane at 15.9 bar. When a limit at the outlet condenser pressure of 0.05 bar is imposed cyclohexane at 20.0 bar is the preferable working fluid. Results show that for the basic case, the overall thermal efficiency of the system is about 56.4%. A maximum efficiency of 62.9% can be obtained by increasing the utilization factor of SOFC to 0.9 and decreasing its current density to 100 A/mm^2. Decreasing the operation temperature of the fuel cells to 650°C lowers the plant efficiency to 55.3%.

Compared to the other technology for conversion of biomass to electric power, the presented plant offers a plant efficiency which is almost double. Comparing a simple ORC with an advanced ORC plant, an improvement of more than 20%-points is obtained. This means that, for a given net power output, the cultivation area required by the system will be

remarkably decreased (around 50%). Further, despite being significantly smaller the present concept competes (in terms of plant efficiency) with other similar plants presented in the literature such as integrated gasification and combined cycle, and integrated gasification with SOFC and steam cycle.

References

[1] Lund H, Mathiesen BV. Energy system analysis of 100% renewable energy systems-The case of Denmark in years 2030 and 2050. J Energy 2009; 34:524–531.

[2] Van de Velden M, Baeyens J, Boukis I. Modeling CFB biomass pyrolysis reactors. Biomass and Bioenergy 2008;32: 128–139.

[3] Coronado CR, Yoshioka JT, Silveira JL. Electricity, hot water and cold water production from biomass. Energetic and economical analysis of the compact system of cogeneration run with woodgas from a small downdraft gasifier. Renewable Energy 2011;36: 1861–1868.

[4] Centeno F, Mahkamov K, Silva Lora EE, Andrade RV. Theoretical and experimental investigations of a downdraft biomass gasifier-spark ignition engine power system. Renewable Energy 2012;37: 97–108.

[5] Pålsson J, Selimovic A, Sjunnesson L. Combined solid oxide fuel cell and gas turbine system for efficient power and heat generation. J Power Sources 2000; 86:442–448.

[6] Proell T, Rauch R, Aichering C, Hofbauer H. Coupling of biomass steam gasification and an SOFC–GT hybrid system for highly efficient electricity generation. ASME Turbo Expo Proceeding 2004. GT2004-53900:103–109.

[7] Subramanyan K, Diwekar U M. Characterization and quantification of uncertainty in solid oxide fuel cell hybrid power plants. J Power Sources 2005; 142:103–116.

[8] Calise F, Dentice d'Accadia M, Vanoli L, von Spakovsky M R. Single-level optimization of hybrid SOFC–GT power plant. J Power Sources 2006;159:1169–1185.

[9] Bang-Møller C, Rokni M, Elmegaard B. Exergy analysis and optimization of a biomass gasification, solid oxide fuel cell and micro gas turbine hybrid system. J Energy 2010; 36:4740–4752.

[10] Dunbar W R, Lior N, Gaggioli R A. Combining fuel cells with fuel – fired power plants for improved exergy efficiency. J Energy 1991; 16(10):1259–1274.

[11] Rokni M, Thermodynamic analysis of an integrated solid oxide fuel cell cycle with a Rankine cycle, J Energy Conversion and Management 2010; 51(12):2724–2732.

[12] Rokni M. Plant characteristics of an integrated solid oxide fuel cell and a steam cycle, J Energy 2010, Vol. 35, 4691–4699.

[13] Rokni M. Thermodynamic investigation of an integrated gasification plant with solid oxide fuel cell and steam cycle. J Green 2012;2:71–86.

[14] Cocco D, Palomba C, Puddu P. Tecnologie delle energie rinnovabili. SGE Editoriali 2010; Padova; ISBN-8889884169.

[15] Drescher U, Brüggemann D. Fluid selection for the organic Rankine cycle (ORC) in biomass power and heat plants. J Applied Thermal Engineering 2007; 27:223–228.

[16] Akkaya V A, Sahin B. A study performance of solid oxide fuel cell-organic Rankine cycle combined system. J Energy Research 2009; 33:553–564.

[17] Al-Sulaiman F A, Dincer I, Hamdullahpur F. Exergy analysis of an integrated solid oxide fuel cell and organic Rankine cycle for cooling, heating and power production. J Power Sources 2010; 195:2346–2354.

[18] Ghirardo F, Santin M, Traverso A, Massardo A. Heat recovery options for onboard fuel cell systems. J hydrogen energy 2011; 36:8134–8142.

[19] Elmegaard B, Houbak N. DNA–A General energy system simulation tool. Proceeding of SIMS 2005; Trondheim, Norway.
[20] Perstrup C. Analysis of power plant installation based on network theory. M.Sc. thesis (in Danish) 1989; Technical University of Denmark, Laboratory of Energetics, Denmark.
[21] Lemmon WE, Huber LM, McLinden OM, NIST reference fluid thermodynamic and transport properties, RFFPROP, version 9.0 user's guide, 2010, Thermophysical Properties Division, National Institute of Standards and Technology, Boulder, Colorado (USA).
[22] Chen H, Goswami Y D, Stefanakos K E. A review of thermodynamic cycles and working fluids for the conversion of low-grade heat. J Renewable and Sustainable Energy Reviews 2010; 14:3059–3067.
[23] Li Y G, Abdul Ghafir M F, Wang L, Singh R, Huang K, Feng X. Nonlinear multiple points gas turbine off-design performance adaptation using a genetic algorithm. ASME J. Eng Gas Turbine Power 2011; 133:071701-1–071701-9.
[24] Smith J M, Van Ness H C, Abbott M M. Introduction to chemical engineering thermodynamics. 7th ed., Boston McGraw-Hill, 2005.
[25] Ahrenfeldt J, Henriksen U, Torben J K, Gøbel B, Wiese L, Kather A, Egsgaard H. Validation of a continuous combined heat and power (CHP) operation of a two-stage biomass gasifier. J Energy and Fuels 2006; 20:2672–2680.
[26] Bang-Møller C, Rokni M. Thermodynamic performance study of biomass gasification, solid oxide fuel cell and micro gas turbine hybrid systems. Energy Conversion and Management 2010;51:2330-9.
[27] Singhal S.C., Kendall K. High temperature solid oxide fuel cells: fundamentals, design and applications. Oxford: Elservier Ltd. ISBN 1856173879. 2003.
[28] Zhu H, Kee R J. A general mathematical model for analyzing the performance of fuel-cell membrane-electrode assemblies. J Power Sources 2003;117:61–74.
[29] Hofmann Ph, Schweiger A, Fryda L, Panopoulos K D, Hohenwarter U, Bentzen J D, et al. High temperature electrolyte supported Ni-GDC/YSZ/LSM SOFC operation on two-stage Viking gasifier product gas. J Power Sources 2007;173:35–366.
[30] Lai N A, Wendland M, Fischer J. Working fluids for high-temperature organic Rankine cycles. Energy 2011; 36:199–211.
[31] Bellomare F, Rokni M. Integration of a municipal solid waste gasification plant with solid oxide fuel cell and gas turbine. Renewable Energy 2013;55:490–500.
[32] DOW Chemical Company. DOWTHERM Q Heat Transfer Fluid. June 1999. http://msdssearch.dow.com/PublishedLiteratureDOWCOM/dh_005f/0901b8038005f2c1.pdf?filepath=heattrans/pdfs/noreg/176-01467.pdf&fromPage=GetDoc.
[33] Pierobon L, Rambabu K, Haglind F. Waste heat recovery for offshore applications. ASME International Mechanical Engineering Congress, November 9-15, Houston, 2012.
[34] Preißinger M, Heberle F, Brüggemann D. Thermodynamic analysis of double-stage biomass fired Organic Rankine Cycle for micro-cogeneration. Int J Energy Res. 2012; 36:944–952.
[35] Prins MJ, Ptasinski KJ, Janssen FJJG. Exergetic optimization of a production process of Fischer-Tropsch fuels from biomass. Fuel Processing Technology 2005;86:375–389.

Nomenclature

Abbreviations

DNA dynamic network analysis
IGSORC integrated gasification, solid oxide fuel cells and organic Rankine cycle
IHE intermediate heat exchanger
HRSG heat recovery steam generator
ORC organic Rankine cycle
SOFC solid oxide fuel cell

Notations

A cultivation area [km^2]
E Nernst voltage [V]
$E_{act,e}$ activation energy for ohmic expression [kJ/kmol]
$\bar{g}_f$ specific Gibbs free energy of formation [kJ/kmol]
H hours of operation [h/year]
h enthalpy [kJ/kg]
$\bar{h}_f$ specific enthalpy of formation [kJ/kmol]
k dimensionless coefficient in Eq. 4
i current density [mA/cm^2]
i_n internal current density [mA/cm^2]
LHV low heating value [kJ/kg or kJ/kmol]
$\dot{m}$ mass flow [kg/s]
P power [kW]
R ideal gas constant [kJ/(kmol K)]
r_e ohmic resistance of electrolyte layer [kΩ/cm^2]
T temperature [K]
U_F utilization factor
ΔV voltage drop [V]

Greek symbols

β annual productivity [ton/ha]
Δ difference of quantities
δ_e electrolyte layer thickness [cm]
η efficiency
σ_e oxygen ion conductivity [S/cm]
$\sigma_{e,o}$ pre-factor of ion conductivity [S/cm]

Subscripts

act activation
aux auxiliary
b biomass
conc concentration polarization
e electrolyte or electric
ohm ohmic polarization
ref reference
rev reversible
th thermal
v voltage

Appendix A

Table A1 lists the thermodynamic properties at the critical point of the working fluids relevant for context of present study. In the table the health hazard (HH), fire hazard (FH) and physical hazard (PH) according to the HMIS (Hazardous Materials Identification System) are also included.

Table A1. Thermodynamic state at critical point and hazard rating for part of the fluids included in DNA library using REFPROP 9. Hazard classification is based on HMIS (Hazardous Materials Identification System) developed by the American Coatings Association.

Fluid	HH*	FH*	PH*	T_c [K]	P_c [kPa]	ρ_{oc} [mol/L]	M_c [g/mol]
1-butane	NA	NA	NA	419.29	4005	4.24	56.11
acetone	2	3	0	508.10	4700	4.70	58.08
air	0	0	0	132.53	3786	11.83	28.97
ammonia	3	1	0	405.40	11333	13.21	17.03
argon	0	0	0	150.69	4863	13.41	39.95
benzene	2	3	0	562.02	4906	3.90	78.11
butane	1	4	0	425.13	3796	3.92	58.12
C1CC6	2	3	0	572.20	3470	2.72	146.70
cis-2-butene	1	4	0	435.75	4226	4.24	134.30
propylcyclohexane	1	2	1	630.80	2860	2.06	126.24
decafluorobutane	1	0	0	386.33	2323	2.52	238.03
dodecafluoropentane	NA	NA	NA	420.56	2045	2.12	288.03
dodecane	2	2	0	658.10	1817	1.33	170.33
trifluoroiodomethane	1	0	0	396.44	3953	4.43	120.00
carbon monoxide	1	4	3	132.86	3494	10.85	28.01
carbon dioxide	1	0	0	304.13	7377	10.62	44.01
carbonyl sulfide	3	4	1	378.77	6370	7.41	60.08
cyclohexane	1	3	0	553.64	4075	3.24	84.16
cyclopentane	2	3	1	511.69	4515	3.82	70.13
cyclopropane	2	2	0	398.30	5580	6.14	42.08
D2	NA	NA	NA	38.34	1665	17.33	4.03
D2O	NA	NA	NA	643.85	21671	17.78	20.03
D4	NA	NA	NA	586.50	1332	1.03	296.62
D5	NA	NA	NA	619.15	1160	0.82	370.77
D6	NA	NA	NA	645.78	961	0.63	444.92
decane	2	2	0	617.70	2103	1.64	142.28
dimethyl carbonate	2	3	0	557.38	4835	3.97	90.08
dimethylether	1	4	2	400.38	5337	5.94	46.07
ethane	1	4	0	305.32	4872	6.86	30.07
ethanol	2	3	0	513.90	6148	5.99	46.07
ethylene	2	4	2	282.35	5042	7.64	28.05
fluorine	4	3	0	144.41	5172	15.60	38.00
hydrogen sulfide	4	4	0	373.10	9000	10.19	34.08

helium	0	0	0	5.20	228	18.13	4.00
heptane	1	3	0	540.13	2736	2.32	100.20
hexane	2	3	0	507.82	3034	2.71	86.18
hydrogen	0	4	0	33.15	1296	15.51	2.02
isobutene	1	4	2	418.09	4010	4.17	56.11
isohexane	2	3	1	497.70	3040	2.72	0.28
isopentane	1	4	0	460.35	3378	3.27	72.15
isobutane	1	4	0	407.81	3629	3.88	58.12
krypton	0	0	0	209.48	5525	10.85	83.80
decamethyltetrasiloxane	1	2	0	599.40	1227	0.91	310.69
dodecamethylpentasiloxane	1	2	0	628.36	945	0.69	384.84
octamethyltrisiloxane	1	2	0	564.09	1415	1.09	236.53
methane	0	4	0	190.56	4599	10.14	16.04
methanol	2	3	0	512.60	8104	8.60	32.04
methyl linoleate	NA	NA	NA	799.00	1314	0.81	294.47
methyl linolenate	NA	NA	NA	722.00	1369	0.85	292.46
hexamethyldisiloxane	2	3	1	518.75	1939	1.59	162.38
methyl oleate	2	1	0	782.00	1246	0.81	296.49
methyl palmitate	1	0	0	755.00	1350	0.90	270.45
methyl stearate	0	1	0	775.00	1239	0.79	298.50
nitrous oxide	1	0	0	309.52	7245	10.27	44.01
neon	0	0	0	44.49	2679	23.88	20.18
neopentane	1	4	0	433.74	3196	3.27	72.15
nitrogen trifluoride	1	0	3	234.00	4461	7.92	71.02
nitrogen	0	0	0	126.19	3396	11.18	28.01
nonane	2	3	0	594.55	2281	1.81	128.26
octane	2	3	0	569.32	2497	2.06	114.23
orthohydrogen	NA	NA	NA	33.22	1311	15.45	2.02
oxygen	0	0	0	154.58	5043	13.63	32.00
parahydrogen	NA	NA	NA	32.94	1286	15.54	2.02
pentane	2	4	0	469.70	3370	3.22	72.15
propane	1	4	0	369.89	4251	5.00	44.10
propylene	1	4	1	364.21	4555	5.46	42.08
propyne	1	4	1	402.38	5626	6.11	40.06
R32	1	4	1	351.26	5782	8.15	52.02
R41	2	3	2	317.28	5897	9.30	34.03
R115	1	0	1	353.10	3129	3.98	173.75
R116	1	0	1	293.03	3048	4.44	173.10
R124	1	1	0	395.43	3624	4.10	261.19
R125	1	1	0	339.17	3618	4.78	120.02
R141B	1	1	0	477.50	4212	3.92	116.95
R142B	1	1	0	410.26	4055	4.44	100.50
R143A	1	1	0	345.86	3761	5.13	84.04
R161	NA	NA	NA	375.30	5091	6.28	48.06
R218	2	1	1	345.02	2640	3.34	188.02
R227EA	NA	NA	NA	374.90	2925	3.50	170.03

R236EA	NA	NA	NA	412.44	3502	3.70	152.04
R236FA	NA	NA	NA	398.07	3200	3.63	152.04
R245CA	NA	NA	NA	447.57	3925	3.91	134.05
R245FA	2	0	1	427.16	3651	3.85	134.05
R365MFC	NA	NA	NA	460.00	3266	3.20	148.07
R507A	1	1	0	343.77	3705	4.96	98.86
R1234YF	1	2	0	367.85	3382	4.17	114.04
R1234ZE	1	2	0	382.52	3636	4.29	114.04
SF6	1	0	0	318.72	3755	5.08	146.06
SO2	3	0	0	430.64	7884	8.20	64.06
trans-butene	0	4	1	428.61	4027	4.21	56.11
toluene	2	3	0	591.75	4126	3.17	92.14
water	0	0	0	647.10	22064	17.87	18.02
xenon	0	0	3	289.73	5842	8.40	131.29
R11	1	0	0	471.11	4408	4.03	137.37
R12	1	0	0	385.12	4136	4.67	120.91
R13	1	0	1	302.00	3879	5.58	104.46
R14	1	0	1	227.51	3750	7.11	88.00
R21	NA	NA	NA	451.48	5181	5.11	102.92
R22	1	1	0	369.30	4990	6.06	86.47
R23	1	1	0	299.29	4832	7.52	70.01
R113	1	0	0	487.21	3392	2.99	187.38
R114	1	0	0	418.83	3257	3.39	170.92
R123	2	1	0	456.83	3662	3.60	152.93
R134A	1	1	0	374.21	4059	5.02	102.03
R152	1	4	1	386.41	4517	5.57	66.05
R404A	1	1	0	345.27	3735	4.94	97.60
R407C	1	1	0	359.35	4632	5.26	86.20
R410	1	1	0	344.49	4901	6.32	72.59
RC318	1	0	2	388.38	2778	3.10	200.03

* Hazard classification is based on HMIS (Hazardous Materials Identification System) developed by the American Coatings Association. It includes health hazard (HH), physical hazard (PH) and fire hazard (FH). The HMIS rating chart ranges from 0 (minimal hazard) to 4 (severe hazard).